JOURNAL OF PHYSICAL ORGANIC CHEMISTRY, VOL. 8, 282–292 (1995)

LIVING CATIONIC POLYMERIZATION OF ISOBUTYL VINYL ETHER BY THE CF_3CO_2H–$SnCl_4$–nBu_4NCl SYSTEM: *IN SITU* DIRECT ANALYSIS OF THE GROWING SPECIES BY ^1H, ^{13}C and ^{19}F NMR SPECTROSCOPY*

HIROSHI KATAYAMA, MASAMI KAMIGAITO,† MITSUO SAWAMOTO‡ AND TOSHINOBU HIGASHIMURA

Department of Polymer Chemistry, Kyoto University, Kyoto 606-01, Japan

Direct ^1H, ^{13}C and ^{19}F NMR spectroscopic analysis was carried out on the carbocationic intermediate generated in the interaction of tin(IV) chloride ($SnCl_4$) with the adduct [4, $CH_3CH(OiBu)OCOCF_3$] of isobutyl vinyl ether (IBVE) and trifluoroacetic acid (CF_3CO_2H), either in the presence or in the absence of tetrabutylammonium chloride. The reactions were to mimic the living cationic polymerization of IBVE by the 4–$SnCl_4$ initiating system (with added nBu_4NCl) that was also found in this study. In CD_2Cl_2 solvent at −78 °C, the ^1H and ^{13}C NMR analysis revealed the formation of a carbocationic intermediate [$CH_3C^+H(OiBu)$] that is in a rapid exchange equilibrium with the covalent counterpart 4. For the first time, the cation formation was further supported by ^{19}F NMR analysis on the counteranionic part (CF_3COO^-) in 4, where, with $SnCl_4$, the CF_3 group gave a broadened signal that appeared clearly downfield relative to that in the covalent form. These and other results, which are in close correlation with the corresponding polymerizations, demonstrated the following: (i) the $SnCl_4$-assisted generation of carbocationic species from the covalent ester 4; (ii) a rapid exchange between the cation and its covalent precursor 4; (iii) the relatively high cationic concentration in the salt-free system, where no living polymerization occurs; and (iv) the effective suppression of the cationic species in the presence of the salt, which proved to be the prime key factor for living polymerization.

INTRODUCTION

Cationic polymerization of vinyl monomers is defined as an addition polymerization reaction where the reactive centre is a cationic intermediate that adds to a monomer molecule by opening the π-bond to form a new cationic centre. As shown in equation (1), the reaction consists of successive electrophilic additions of the polymeric growing cation, derived from an initiator and a monomer, to remaining monomers. If each addition reaction occurs without such undesirable reactions as chain transfer and termination, it consists only of initiation and propagation and is thereby called as living polymerization. In general, however, the growing carbocations are highly reactive but unstable and subject to a number of side-reactions [equation (2)], and it has long been considered almost impossible to prepare polymers with controlled structures by cationic vinyl polymerization. This had been in contrast to long-known living anionic[3] and cationic ring-opening[4] polymerizations where the intermediates are more stable carbanions and oxonium cations, respectively.

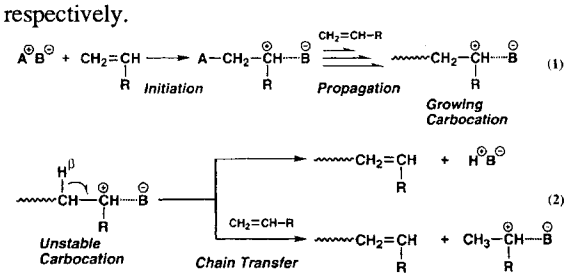

However, such a view on cationic vinyl polymerizations proved to be wrong when the living cationic

*This work was presented in part at the 42nd Annual Meeting of the Society of Polymer Science, Tokyo, Japan, September 1993, paper 20D15[1] and at the International Conference on Frontiers in Polymerization, Liège, Belgium, October 1993.[2]

† Research Fellow of the Japan Society for the Promotion of Sciences.

‡ Author for correspondence.

CCC 0894–3230/95/040282–11

Received 16 August 1994
Revised 20 October 1994

polymerization of vinyl ethers was accomplished with the use of a mixture of hydrogen iodide and iodine or the HI–I_2 initiating systems.[5] Since then, a large number of living cationic polymerizations have been found for various monomers including vinyl ethers, isobutene and styrenes.[6] Most of the initiating systems for these living polymerizations are composed of two components, a cationogen (initiator) such as a protonic acid (HB), reactive alkyl chloride or acetate, and a metal halide or Lewis acid (activator; MX_n). As illustrated schematically in equation (3),

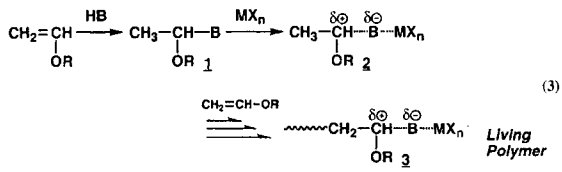

(3)

for example, the initial reaction is the quantitative electrophilic addition of HB to a vinyl monomer to form an adduct (**1**), the C′–B bond of which is then electrophilically activated by MX_n into species **2**. This activated form of **1** is the actual initiating entity that commences the living propagation subsequently mediated via its polymeric homologue (**3**).

To achieve living cationic polymerization, a judicious choice of initiating systems is important. Why, then, do these specific initiating systems induce controlled or living polymerizations via supposedly cationic intermediates which have been considered unstable? Although it appears true, as we have repeatedly pointed out,[6a,c] that nucleophilic interaction of counteranions or occasionally added bases or salts with the growing carbocation is of primary importance, it is still not fully understood and often controversial what the nature of the living propagating species is, and whether or not there is a difference between living and non-living species.[7]

To clarify these points, it would be of interest to analyse model growing species [**2**; equation (3)], *in situ*, directly, and spectroscopically, under the conditions mimicking the actual living polymerizations. Thus, by ^1H and ^{13}C NMR spectroscopy we have recently analysed the model growing species in the living cationic polymerization of isobutyl vinyl ether (IBVE) by the HCl–$ZnCl_2$ and HCl–tin(IV) chloride ($SuCl_4$)–tetrabutylammonium chloride (nBu_4NCl).[8–10] As shown in equation (3), the living growing end (**2** and **3**) should consist of three components, the growing carbocation (∼∼C^+) from the monomer, the counteranion (B^-) from the initiator HB and the activator (MX_n) associating with B^-. Our NMR analysis was in fact directed toward only one of these three, i.e. the carbocationic part. Those studies demonstrated that a carbocationic intermediate is indeed generated from the HCl adduct (**1**; B = Cl) of IBVE and a Lewis acid and that the concentration of the ionic species is very low under the conditions where living polymerization occurs. However, the interaction between the counteranion and the carbocation remained unclear, because the HCl-based systems inherently fail to permit the NMR analysis of the counteranionic part, or the chloride anion.

To analyse the growing species more comprehensively, therefore, in this study we employed trifluoroacetic acid (CF_3CO_2H) as an initiator in conjunction with a Lewis acid (MX_n: $SnCl_4$ and $ZnCl_2$) for IBVE polymerization. The counteranionic parts to be generated in these systems contain not only a ^{13}C but also a ^{19}F nucleus, which has a spin number of 1/2 and a high sensitivity to NMR (the overall sensitivities are 0·83 and 4700 relative to ^1H and ^{13}C, respectively). This system thereby permits the direct analysis of not only the carbocationic part by ^1H and ^{13}C NMR but also the counteranionic part by ^{19}F and ^{13}C NMR [equation (4)].

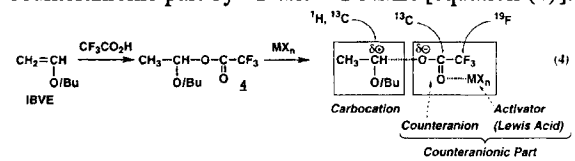

(4)

In the first part of this study, we investigated the polymerization of IBVE by CF_3CO_2H in conjunction with $ZnCl_2$ and $SnCl_4$. As does hydrogen chloride,[8–10] CF_3CO_2H forms an ester **4** with IBVE, but **4** would initiate polymerizations of IBVE when coupled with an appropriate Lewis acid. In fact, we have already reported that the **4**–$ZnCl_2$ system induces living cationic polymerization of IBVE in toluene.[8] In this study, polymerizations by **4** in conjunction with not only $ZnCl_2$ but also a stronger Lewis acid, $SnCl_4$, were carried out in CH_2Cl_2 to investigate the effects of the Lewis acidity of metal halides. The second part concerned *in situ* ^1H, ^{13}C and ^{19}F NMR analysis of model growing terminals generated from **4** and these two activators, especially focusing on the analysis of the counteranionic part and the effects of ester fragments, counteranions, and Lewis acids.

RESULTS AND DISCUSSION

Living cationic polymerization

Trifluoroacetic acid (CF_3CO_2H) reacts quantitatively with IBVE to form adduct **4** with a covalent ester bond, which is incapable of initiating polymerization (see Experimental).[8] However, IBVE was polymerized with **4** in conjunction with $ZnCl_2$ and $SnCl_4$.

As shown in Figure 1, quantitative polymerization occurred with a weak Lewis acid, $ZnCl_2$. In contrast, the system with $SnCl_4$, a stronger Lewis acid, induced an almost instantaneous, extremely rapid, and thereby uncontrollable polymerization. Therefore, we added to this system nBu_4NCl, which is effective in inducing the

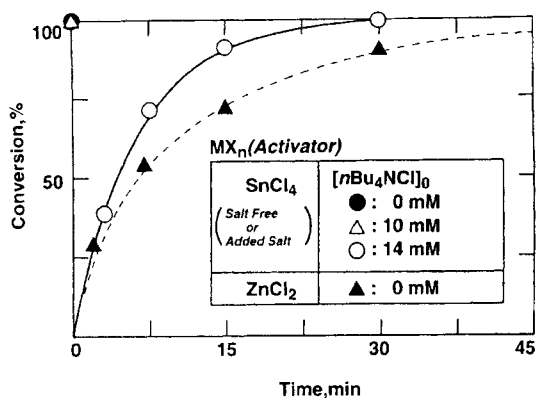

Figure 1. Time–conversion curves for the polymerization of IBVE with 4–MX_n in the absence and the presence of nBu_4NCl in CH_2Cl_2 at −15 °C. $[Monomer]_0$ ($[M]_0$) = 1·0 M; [4 (initiator)]$_0$ = 20 mM; $[MX_n$ (activator)]$_0$ = 10 mM; [nBu_4NCl (added salt)]$_0$ as indicated

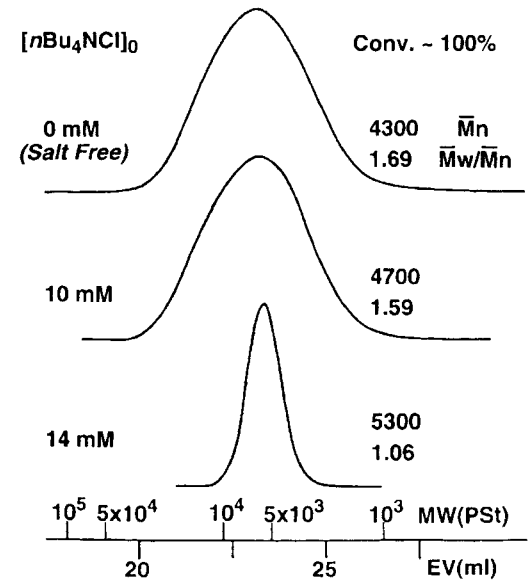

Figure 2. Effects of added nBu_4NCl on the IBVE polymerization with 4–$SnCl_4$ in CH_2Cl_2 at −15 °C. $[M]_0$ = 1·0 M; [4]$_0$ = 20 mM; $[SnCl_4]_0$ = 10 mM; [nBu_4NCl]$_0$ = 0, 10 and 14 mM

living polymerization of IBVE by the HCl–$SnCl_4$ initiating system. Although the polymerization in the presence of nBu_4NCl equimolar with respect to $SnCl_4$ (10 mM) was still rapid, a higher salt concentration (14 mM) led to a slower polymerization that was similar in rate to the $ZnCl_2$-mediated counterpart without the salt.

Figure 2 shows the molecular weight distribution (MWD) curves of the polymers obtained with the 4–$SnCl_4$ initiating system at varying salt concentrations. The polymers obtained in the absence of nBu_4NCl had a broad MWD, and so did that in the presence of nBu_4NCl equimolar with respect to $SnCl_4$ ($\bar{M}_w/\bar{M}_n \approx 1{\cdot}6$). However, with use of a slightly larger amount of nBu_4NCl, the MWD became very narrow ($\bar{M}_w/\bar{M}_n \leq 1{\cdot}1$).

Figure 3 plots the number-average molecular weights ($\bar{M}_n$) of polymers against monomer conversion for the polymers obtained with either $ZnCl_2$ (salt free) or $SnCl_4$ (with 14 mM nBu_4NCl). In both cases, the $\bar{M}_n$ increased in direct proportion to conversion and agreed with the calculated values assuming that one molecule of **4** generates one living polymer chain. Therefore, despite the difference in the narrowness in polymer MWD, the 4–$SnCl_4$ system induces living polymerization of IBVE in the presence of nBu_4NCl, whereas a weaker Lewis acid, $ZnCl_2$, also gives a similar living polymerization even without nBu_4NCl (Scheme 1). The broader MWD with $ZnCl_2$ is apparently due to the slow interconversion between the dormant species and the activated species (the more rapidly the interconversion between the activated (ionic) species and the dormant (covalent) species occurs under the condition of living cationic polymerization, the narrower the MWD of the obtained polymer becomes; the effects of the rate of such inter-conversion on the polymer MWD have been discussed[11]). These results for the CF_3CO_2H adducts (**4**) are very similar to those with the adduct of HCl as an initiator.[7] However, the overall polymerization rates with **4** were much smaller than those with the HCl-based systems, owing to the stronger C—$OCOCF_3$ linkage than the C—Cl bond.

Direct NMR analysis of model reactions

To clarify the nature of the growing species in the CF_3CO_2H-mediated polymerizations, the interaction of **4** with MX_n (MX_n = $SnCl_4$ and $ZnCl_2$) was directly analysed by ^1H, ^{13}C and ^{19}F NMR spectroscopy, especially focusing on the counteranionic part formed from trifluoroacetate anion ($CF_3CO_2^-$) and MX_n. Here **4** is considered as the simplest model of the growing polymer terminal in the 4–MX_n-initiated polymerization. ^1H, ^{13}C and ^{19}F nuclei were monitored under identical conditions, so that their spectral correlations could be discussed.

In this section, we investigated the following in relation to the polymerization results discussed above: (1) *in situ* direct observation of the carbocation and the counteranionic part generated from the adduct **4** by ^1H, ^{13}C and ^{19}F NMR spectroscopy; (2) the relationships between the NMR spectra of the model reactions and the living character of the corresponding polymerizations; (3) the effects of the nucleophilicity of the counteranionic part on the living polymerizations.

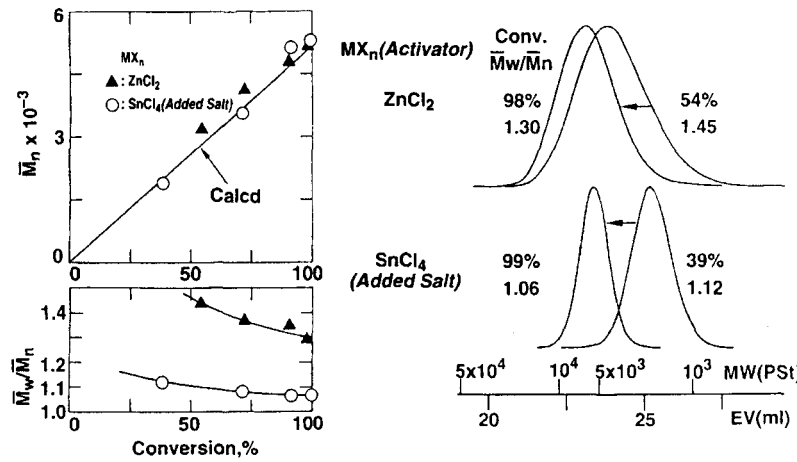

Figure 3. Living polymerization of IBVE with (△) **4**–$ZnCl_2$ or (○) **4**–$SnCl_4$ in the presence of nBu_4NCl in CH_2Cl_2 at −15 °C. $[M]_0 = 1{\cdot}0$ M; $[\mathbf{4}]_0 = 20$ mM; $[ZnCl_2]_0 = 10$ mM, $[SnCl_4]_0/[nBu_4NCl]_0 = 10/14$ mM. The 'Calcd' solid line indicates the calculated $\bar{M}_n$ assuming the formation of one living polymer per molecule of **4**

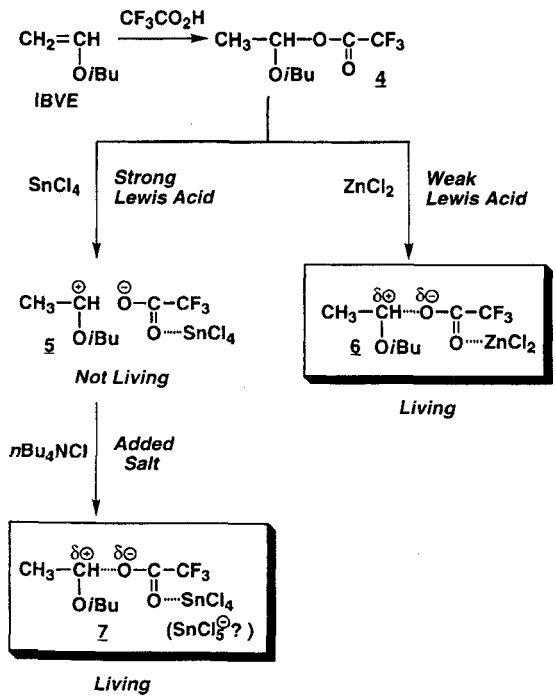

Scheme 1

Because the counteranionic part is composed of the counteranion (B^-) from the initiator HB (or adduct **4**) and the Lewis acid activator (MX_n), not only the basicity of B^- but also the acidity of MX_n would determine its overall nucleophilicity, which will seriously affect the nature of the growing species. Thus, we studied the effects of B^- and those of MX_n separately.

*In situ ^{13}C and ^{19}F NMR analysis of the counter anion (B^-) in the **4**–$SnCl_4$ system: evidence for the generation of carbocationic species*

Figure 4 shows the ^1H, ^{13}C and ^{19}F NMR spectra of the mixtures of the **4** and $SnCl_4$ in the absence and the presence of nBu_4NCl in CD_2Cl_2 at −78 °C where the concentration of **4** is constant ($[\mathbf{4}]_0 = 200$ mM). As shown in Figure 4(A) for **4** alone, the signal of the α-methine *b* (—*CH*—*O*—), which is adjacent to the ester moiety, appeared at 102 ppm in ^{13}C NMR and at 6·0 ppm in ^1H NMR as a sharp quartet. The two protons c_1 and c_2 of the pendant methylene adjacent to the ether oxygen (—OCH_2—) are chemical shift non-equivalent owing to the asymmetric α-carbon to give a pair of resonances around 3·3 ppm (doublets of doublets).

On mixing $SnCl_4$ to a cooled solution of **4** under salt-free conditions [Figure 4(B) and (C)], the spectra changed clearly: the methine proton (H^b) and carbon (C^b) both shifted downfield and broadened, and the higher the $SnCl_4$ concentration the greater were the downfield shifts. Along with these changes, the initially separate methylene proton resonances coalesced into a sharp doublet and also shifted downfield. These spectral changes show that the covalent C—$OCOCF_3$ bond in **4** is polarized by $SnCl_4$ to give carbocationic species (**5**), that it is in a rapid exchange equilibrium with the covalent precursor **4** and that the higher the $SnCl_4$ concentration, the higher is the cation concentration. [As will be mentioned later, the observation from the side of the carbocation in part by ^1H and ^{13}C NMR shows that the extent of the downfield shift of the α-

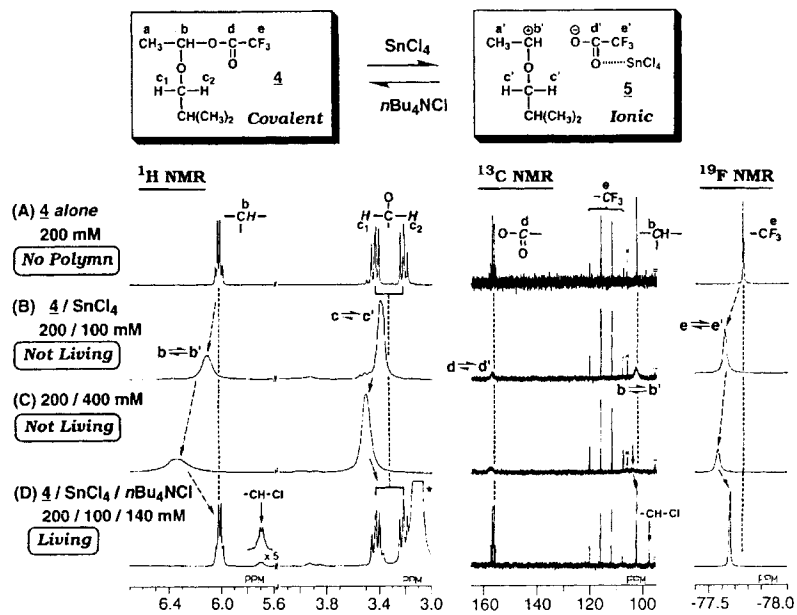

Figure 4. ^1H, ^{13}C and ^{19}F NMR spectra of (A) **4** and (B–D) mixtures of **4** and $SnCl_4$ in the absence and the presence of nBu_4NCl in CD_2Cl_2–CCl_4 (4:1) at −78 °C with varying $SnCl_4$ concentration. $[\mathbf{4}]_0 = 200$ mM; $[SnCl_4]_0$ and $[nBu_4NCl]_0$ as indicated. The asterisked signal is for the α-methylene protons in the salt $[(CH_3CH_2CH_2CH^*_2)_4NCl]$

methine of the HB–IBVE adducts is smaller in **4** (—B = —$OCOCF_3$) than in **10** (—B = —Cl), which indicates that the concentration of the carbocationic species from **4** is lower (see Figures 8 and 9).]

On the other hand, the signals of the counteranion ($CF_3CO_2^-$) from **4** are seen in the ^{13}C and ^{19}F NMR spectra. For **4** alone [Figure 4(A)], the carboxyl carbon *d* (—*O*C*O*—) and the trifluoromethyl carbon *e* (—*C*F_3) appeared in ^{13}C NMR at 157 and 114 ppm, respectively, both as sharp quartets owing to the ^{13}C–^{19}F spin–spin coupling. In ^{19}F NMR, the signal of CF_3 group *e* appeared at −77·75 ppm as a sharp singlet. After the $SnCl_4$ addition [Figure 4(B) and (C)], along with the changes in the α-methine signal *b* (see above), all of the carboxyl carbon *d* in ^{13}C NMR and the CF_3 *e* in ^{19}F NMR shifted downfield and broadened, which shows the generation of the anion $CF_3CO_2^-$. The broadness of these peaks also indicates a rapid exchange between the carbocationic species **5** and its covalent precursor **4**. Thus, the carbocation formation has demonstrated by monitoring not only the carbocationic component of a model growing species by ^1H and ^{13}C NMR but also the counteranionic component by ^{13}C and ^{19}F NMR. These results suggest the participation of the carbocationic intermediate **5** in the **4**–$SnCl_4$-initiated polymerization, because polymerizations do not occur until the covalent precursor **4** is mixed with $SnCl_4$. Importantly, however, under these conditions, the IBVE polymerization is not living (cf. Figure 2).

When a sufficient amount of nBu_4NCl was additionally mixed to the mixture of **4** and $SnCl_4$ [Figure 4(D)], under which condition living cationic polymerization occurred (Figures 2 and 3), both the methine proton (H^b) and carbon (C^b) returned to the original upfield positions for **4** alone and became sharp again, which indicates the suppression of the ionic species **5** by adding the salt. The salt addition also led to a new signal, the quartet at 5·7 ppm in the ^1H NMR spectrum and the sharp singlet at 97 ppm in ^{13}C NMR spectrum that are assigned to the α-methine of HCl–IBVE adduct (**10** in Figures 8 and 9). The formation of a small amount of **10** indicates the anion exchange between $CF_3CO_2^-$ from **4** and the chloride anion (Cl^-) from nBu_4NCl and/or $SnCl_4$, which in turn supports further that even under the salt-present condition, the carbocationic species was actually generated, although at an extremely low concentration. The CF_3 resonance *e* in ^{19}F NMR also returned toward the original position and also sharpened. Thus, the suppression of the ionic species by adding the salt was confirmed by the observation of not only the carbocation (^1H and ^{13}C NMR) but also the counteranion (^{13}C and ^{19}F NMR). Close inspection of the ^{19}F NMR spectrum in Figure 4(D) also revealed that the CF_3 signal *e* is still slightly downfield relative to that for the covalent precursor **4** alone [Figure 4(A)]. This slight difference between the spectra for the covalent form **4** and the salt-suppressed ion (**4** ⇌ **5**) was not detectable by ^1H and ^{13}C NMR,

and the highly sensitive ^{19}F NMR analysis proved effective in distinguishing these two systems.

The slight downfield shift of the CF_3 signal may indicate coordination of $SnCl_4$ to the ester moiety of **4**, even in the presence of the salt. To understand such an interaction more clearly, ^{19}F NMR spectra were taken for a series of mixtures of $SnCl_4$ and covalent or ionic trifluoroacetates (Figure 5). Figure 5(C) is the spectrum of $nBu_4N^+CF_3CO_2^-$ (**8**), which is considered as a model of the anion $CF_3CO_2^-$ alone; the CF_3 signal appeared as a sharp singlet at −77·09 ppm, clearly more downfield than did the covalent species **4** [Figure 5(A); −77·75 ppm]. The observed difference also supports that the downfield shift and its broadening of the CF_3 signals is due to the generation of the counteranionic part (and the carbocation) in the **4**–$SnCl_4$ system [Figure 5(B)]. When $SnCl_4$ was mixed with **8** [Figure 5(D)], where a $CF_3CO_2^-$–$SnCl_4$ complex or a pentacoordinated tin anion $[CF_3CO_2\text{-}SnCl_4]^-$ would arise, the CF_3 signal in fact appeared as a sharp singlet at a much more downfield position (−75·30 ppm), near the signal of silver trifluoroacetate ($CF_3CO_2^-Ag^+$) [Figure 5(E); −75·01 ppm]. The two highly downfield signals show that the existence of an electron-deficient metal

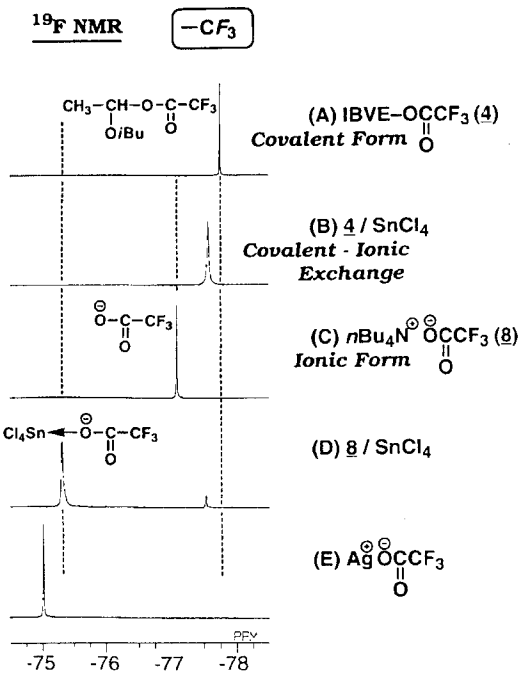

Figure 5. ^{19}F NMR spectra of (A) **4** (B) **4**–$SnCl_4$, (C) **8**, (D) **8**–$SnCl_4$ and (E) $Ag^+CF_3CO_2^-$ at −78 °C. (A) and (B) in CD_2Cl_2–CCl_4 (4 : 1); $[\mathbf{4}]_0 = 200$ mM; $[SnCl_4]_0 = 400$ mM. (C) and (D) in CD_2Cl_2; $[\mathbf{8}]_0 = 200$ mM (C), $[\mathbf{8}]_0/[SnCl_4]_0 = 100/100$ mM (D). (E) in toluene-d_8; $[Ag^+CF_3CO_2^-]_0 = 200$ mM

around $CF_3CO_2^-$ causes a downfield shift of the ^{19}F signal of $CF_3CO_2^-$. It follows that the signal of the counteranionic part (schematically $CF_3CO_2^-\cdots SnCl_4$) to be formed from the **4**–$SnCl_4$ system would appear around −75 ppm, but the signal [Figure 5(B)] is actually detected at a more upfield position, and the CF_3 chemical-shift difference between **4** and **4**–$SnCl_4$ is clearly smaller than that between **4** and **8**–$SnCl_4$ [Figure 5(D)]. Thus, the ionization efficiency of the **4**–$SnCl_4$ pair is relatively low (see earlier comment in brackets), but the generation of the ionic species in even such a small amount makes the control of IBVE polymerization difficult (cf. Figure 2).

Apart from the carbocation formation from **4**, the small downfield ^{19}F NMR shift in the **4**–$SnCl_4$ system might simply be due to a loose coordination of $SnCl_4$ to the ester carbonyl in **4**, as often observed for other carboxylate–metal halide mixtures. To test this possibility, the interaction of $SnCl_4$ and ethyl trifluoroacetate ($CF_3CO_2C_2H_5$; **9**) was analysed by ^1H and ^{19}F NMR spectroscopy (Figure 6). Obviously, the primary ester could hardly be ionized into an ethyl cation by $SnCl_4$. On mixing **9** and $SnCl_4$ [Figure 6(B)], the methylene and the CF_3 resonances indeed shifted downfield slightly but without broadening, and the shift was much smaller than in the **4**–$SnCl_4$ system. Therefore, $SnCl_4$ does coordinate to **9** but cannot induce any ion–ester exchange. Separate experiments also showed the absence of IBVE polymerization by **9**–$SnCl_4$. Thus, these spectral observations with **9** further support the participation of the ionic species **5** in the **4**–$SnCl_4$-initiated polymerization.

In the ^1H and ^{19}F NMR spectra of the **9**–$SnCl_4$–nBu_4NCl system [Figure 6(C)], no downfield shifts were observable, where the salt most likely weakens the coordination of $SnCl_4$ to the ester by forming a weaker Lewis acid, $SnCl_5^-$.

^1H and ^{19}F NMR analysis of the **4**–$ZnCl_2$ *system: effects of Lewis acids* MX_n

Not only the use of $SnCl_4$ with added nBu_4NCl but also that of a weak Lewis acid, $ZnCl_2$, without the salt permit living polymerization of IBVE with **4** (Figure 3). The interaction of **4** and $ZnCl_2$ was therefore investigated by ^1H and ^{19}F NMR spectroscopy (Figure 7). As shown in Figure 7(D), the α-methine signal *b* in the ^1H NMR spectrum appeared almost at the original position for **4** alone [Figure 7(A)], and the CF_3 signal *e* in the ^{19}F NMR spectrum shifted slightly downfield but remained sharp. Thus, with a weak acid, $ZnCl_2$, as an activator, the generation of the ionic species was kept at an extremely low concentration even in the absence of nBu_4NCl, and the spectra for the **4**–$ZnCl_2$ [Figure 7(D)] and the **4**–$SnCl_4$–nBu_4NCl [Figure 7(C)] systems are very similar; note that both systems lead to living IBVE polymerization. A very small peak at

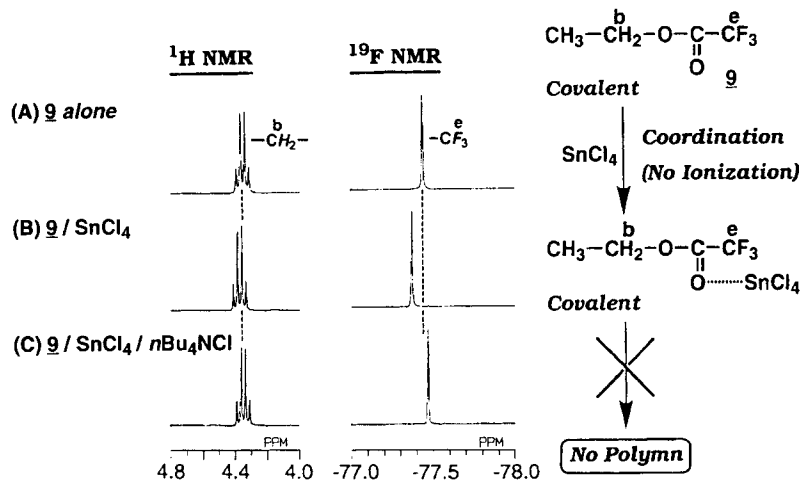

Figure 6. Interaction of ethyl trifluoroacetate (**9**) with $SnCl_4$ and nBu_4NCl in CD_2Cl_2–CCl_4 (4 : 1, v/v) at −78 °C followed by ^{1}H and ^{19}F NMR spectroscopy. (A) **9** alone; (B) **9**–$SnCl_4$; (C) **9**–$SnCl_4$–nBu_4NCl. [**9**] = 200 mM; [$SnCl_4$] = 100 mM; [nBu_4NCl] = 140 mM

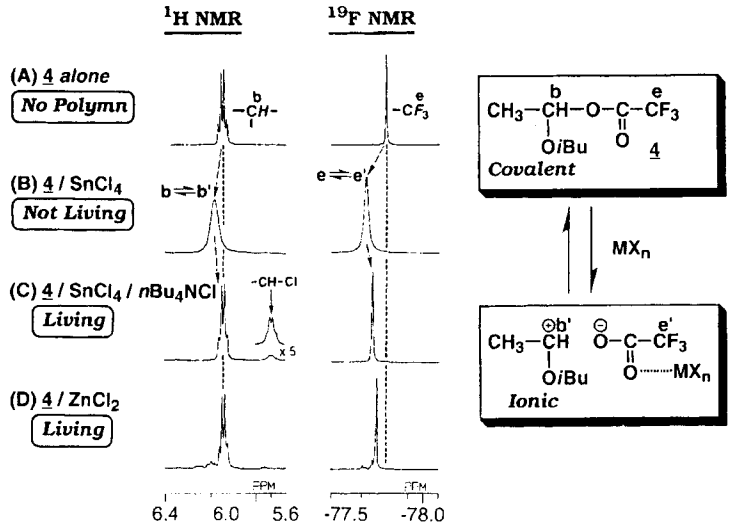

Figure 7. Effects of Lewis acids (MX_n) and added nBu_4NCl on the ^{1}H and ^{19}F NMR spectra of **4**–MX_n mixtures in CD_2Cl_2 at −78 °C. (A) **4** alone; (B) **4**–$SnCl_4$; (C) **4**–$SnCl_4$–nBu_4NCl; (D) **4**–$ZnCl_2$ [with 10 vol.% Et_2O from the stock solution of $ZnCl_2$ (it has already been shown[8] that diethyl ether, i.e. the solvent for $ZnCl_2$, does not affect the nature of living polymerization)]. [**4**] = 200 mM; [$SnCl_4$] = [$ZnCl_2$] = 100 mM; [nBu_4NCl] = 140 mM

5·74 ppm in Figure 7(D) indicates the formation of the HCl–IBVE adduct (**10**) due to the counteranion exchange, as also observed in the **4**–$SnCl_4$–nBu_4NCl system.

Relationships between living cationic polymerization and the NMR spectra of the model reactions

The above-discussed results demonstrate a close correlation between the living nature of the IBVE polymerizations with **4** and the NMR spectra of the corresponding model reactions. For example, in the observation of the carbocationic component by ^{1}H and ^{13}C NMR (Figures 4 and 7), the extensive downfield chemical shifts of the α-methine signal *b* in the **4**–$SnCl_4$ system [salt free; Figure 7(B)] indicate that a relatively high concentration of the carbocationic species is unfavourable for living polymerization. In contrast, when the cation is hardly observable as in the **4**–$SnCl_4$–nBu_4NCl [Figure 7(C)] and the **4**–$ZnCl_2$

[Figure 7(D)] systems, living polymerizations occur. Similar relationships have been found between the IBVE polymerizations with the HCl–IBVE adduct (**10**) and the NMR spectra of relevant model reactions (see Figures 8 and 9; Refs 9 and 10). Thus, to achieve living cationic polymerization, it is important to suppress carbocationic growing species at an extremely low concentration below the NMR detection limits.

A similar correlation was seen in the observation of the counteranionic component by ^{19}F and ^{13}C NMR. The CF_3 resonance *e* shifted downfield in the salt-free **4**–$SnCl_4$ system [Figure 7(B)], which gave non-living polymers. It appeared very close to the downfield position for the CF_3 of **4** alone in the **4**–$SnCl_4$–nBu_4NCl [Figure 7(C)] and the **4**–$ZnCl_2$ [Figure 7(D)] systems, under which conditions living polymerizations proceeded. The ^{19}F NMR analysis also demonstrated that $SnCl_4$ actually interacts (coordinates) with $CF_3CO_2^-$ in both living and non-living polymerizations.

CF_3CO_2H–$SnCl_4$ vs HCl–$SnCl_4$ systems: effects of counteranions (B^-)

We have recently reported that the HCl–$SnCl_4$ initiating system induces living cationic polymerization of IBVE in the presence of nBu_4NCl.[9] The HCl-based system is similar to the CF_3CO_2H-based counterpart discussed here, except for the difference in the counteranions B^- in the protonic acids. The difference in turn permits us to examine the effects of B^- on the nature of growing species. Figures 8 and 9 show the ^1H and ^{13}C NMR spectra, respectively, of model reaction mixtures [HB–IBVE adduct (**4** or **10**) + $SnCl_4$ + nBu_4NCl] corresponding the two initiating systems. Overall results are also summarized in Table 1. When adducts **4** (—B = —$OCOCF_3$) and **10** (—B = —Cl) were mixed with $SnCl_4$ in the absence of the salt [Figures 8(B) and 9(B)], both α-methine signals *b* shifted downfield; the downfield shift with **4** is much smaller than with **10**, indicating that the concentration of the ionic species generated from **4** is much lower than that from **10**. This suggests that the C—$OCOCF_3$ bond in **4** is more difficult to ionize than the C—Cl bond in **10**, which is consistent with the larger pK_a of CF_3CO_2H than of HCl, as shown in Table 1. Thus, it has been clarified by the direct NMR investigations that the property of the counteranionic part ($B^-\cdots MX_n$) is influenced not only by the Lewis acidity of MX_n but also by the basicity of B^-; both factors, in turn, affect the instantaneous concentration of the carbocationic species.

In the presence of nBu_4NCl, where the living polymerizations proceeded with both initiating systems, the α-methine signals returned to the original upfield positions for the respective adducts [Figures 8(C) and 9(C)]. Importantly, the non-equivalent methylene proton signals c_1 and c_2 of **10** coalesced into a sharp doublet, whereas those of **4** remained split resonances. This indicates that the covalent–ionic exchange in **4**–$SnCl_4$ is slower than that in **10**–$SnCl_4$, which may be caused by the fact that the rate-determining step of the exchange reaction is the generation of the ionic species by disrupting the C—B bond with $SnCl_4$. Hence these direct

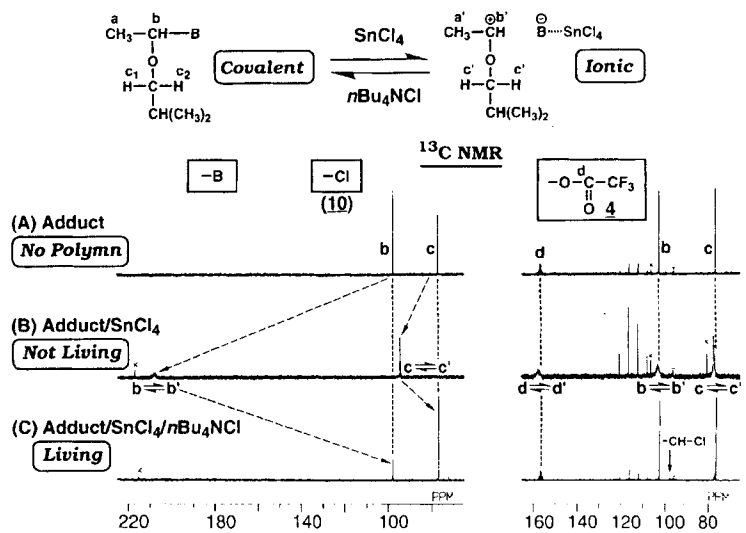

Figure 8. Effects of counteranion (B^-) on ^1H NMR spectra of HB–IBVE adducts (**4** and **10**) with $SnCl_4$ in CD_2Cl_2 at −78 °C. (A) adduct alone (**4**, –B = –Cl; **10**, –B = –$OCOCF_3$) with 20 vol.% CCl_4 from the stock solutions of the adducts; (B) adduct–$SnCl_4$; (C) adduct–$SnCl_4$–nBu_4NCl. [Adduct] = 200 mM; [$SnCl_4$] = 100 mM; [nBu_4NCl] = 140 mM. The asterisked signals are for the α-methylene protons in the salt [$(CH_3CH_2CH_2CH^*_2)_4NCl$]

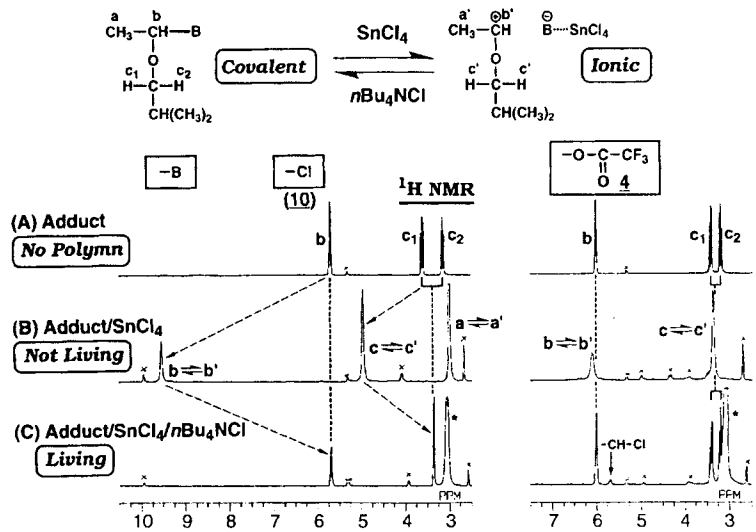

Figure 9. Effects of counteranion (B^-) on ^{13}C NMR spectra of HB–IBVE adducts (**4** and **10**) with $SnCl_4$ in CD_2Cl_2 at −78 °C. (A) adduct alone (**4**, –B = –Cl; **10**, –B = –$OCOCF_3$) with 20 vol.% CCl_4 from the stock solutions of the adducts; (B) adduct–$SnCl_4$; (C) adduct–$SnCl_4$–nBu_4NCl. See the caption for Figure 8 for detailed conditions

Table 1. Effects of counteranions (B^-) on the IBVE polymerization and the corresponding model reactions

HB	IBVE polymerizations[a]			Model reactions (NMR analysis)[b]			
				C^+concentration			
	$MX_n = SnCl_4$ (salt free)	$MX_n = SnCl_4$ (added salt)	$MX_n = ZnCl_2$ (salt free)	Salt free	Added salt	Covalent–ionic exchange	Anion basicity (pK_a in DMSO)[c]
HCl[d]	A	B	B	High	Very low	Faster	1·8
$HOC(O)CF_3$[e]	A	B	C	Low	Very low	Slower	3·45

[a] Polymerization of IBVE with the HB–IBVE adduct–MX_n initiating system. (A) instantaneous polymerization, not living; (B) living, very narrow MWD ($M_w/M_n < 1·1$); (C) living, broad MWD.
[b] *In situ* NMR analysis of model reactions with the HB–IBVE adduct–$SnCl_4$ at −78 °C. Reaction conditions: HB = HCl, in CD_2Cl_2; HB = CF_3CO_2H, in CD_2Cl_2–CCl_4 (4 : 1, v/v). [Adduct] = 200 mM; [$SnCl_4$] = 100 mM; [nBu_4NCl] = 140 mM (see Figures 8 and 9).
[c] Ref. 12.
[d] IBVE was polymerized in CH_2Cl_2 at −15 °C: $[M]_0 = 0·38$ M; $[\mathbf{10}]_0 = 5$ mM; $[MX_n]_0 = 2$ mM; $[nBu_4NCl]_0 = 2–4$ mM.[9]

NMR analysis of the model reactions also clarified that the counteranion affects not only the ease of the ionization of the C—B terminus by MX_n but also the rate of the covalent–ionic exchange.

EXPERIMENTAL

Materials. IBVE (Tokyo Kasei; purity >99%) was washed with 10% aqueous sodium hydroxide solution and then with water, dried overnight with potassium hydroxide (pellets) and distilled twice over calcium hydride before use. CF_3CO_2H (Nacalai Tesque; purity >99%), commercially received in sealed vials, was dissolved in toluene or carbon tetrachloride (CCl_4) without further purification. $SnCl_4$ (Wako Chemicals; purity >97%) was distilled under reduced pressure over phosphorus pentoxide. $ZnCl_2$ (Aldrich; 1·0 M solution in diethyl ether) was commercially supplied as a solution. nBu_4NCl (Tokyo Kasei) was used as received. It was vacuum dried just before use and dissolved in dry and distilled methylene chloride in a nitrogen-filled dry-box. Deuterated methylene chloride (CD_2Cl_2) (Wako Chemicals; 99·75 atom% D) and toluene-d_8 (Aldrich; >99 atom% D) were dried overnight over baked molecular sieves 3Å just before use. Methylene chloride (CH_2Cl_2) and carbon tetrachloride (CCl_4) as solvents were washed with 10% aqueous sodium hydroxide and then with water, dried overnight with calcium chloride and doubly distilled over phosphorus pentoxide and then over calcium hydride before use.[4] Diethyl ether (Et_2O) (Dojin; purity >99%, anhydrous) for $ZnCl_2$ solution was distilled in the presence of $LiAlH_4$ before use. Silver

trifluoroacetate ($AgOCOCF_3$) (Aldrich; purity >98%) was vacuum dried and dissolved in toluene-d_8 before use. Ethyl trifluoroacetate ($CF_3CO_2C_2H_5$; **9**) (Wako Chemicals; purity >98%) was used as received.

*Synthesis of CF_3CO_2H–IBVE adduct (**4**).*[8] The adduct **4** was synthesized by magnetically stirring a mixture of CF_3CO_2H and IBVE in toluene at 0 °C (for polymerization initiator) or in CCl_4 at 0 °C (for model reactions). The clean and quantitative formation of the adduct in both solvents was confirmed by ^1H and ^{13}C NMR spectroscopy. The HCl adduct **10** was prepared similarly.[9]

Synthesis of tetrabutylammonium trifluoroacetate ($nBu_4NOCOCF_3$). This salt was prepared by adding a solution of $AgOCOCF_3$ in toluene (25%, w/v; 19 ml) to a solution of nBu_4NCl in CH_2Cl_2 (10%, w/v; 60 ml) at room temperature. After stirring for 10 min, the precipitated silver chloride was filtered off. The product was isolated by evaporating the solvents under reduced pressure and purified by reprecipitation from dry, distilled *n*-hexane to give the trifluoroacetate as a white powder; yield 74% from $AgOCOCF_3$. It was vacuum dried and dissolved in dry and distilled CH_2Cl_2 in a nitrogen-filled dry-box just before use.

Polymerization procedures. Polymerization was carried out under dry nitrogen in baked glass tubes equipped with a three-way tap. The reaction was initiated by the sequential addition of prechilled solutions of **4** (in toluene; 0·50 ml) and $SnCl_4$ (in CH_2Cl_2; 0·50 ml) or $ZnCl_2$ (in Et_2O; 0·50 ml) via dry syringes into a monomer solution (in CH_2Cl_2; 4·0 ml) containing IBVE (0·66 ml) and CCl_4 (0·20 ml). For polymerizations in the presence of nBu_4NCl, the salt was dissolved in $SnCl_4$ solution prior to initiation. After predetermined intervals, the polymerization was terminated with prechilled methanol (2·0 ml) containing a small amount of ammonia. Monomer conversion was determined from its residual concentration measured by gas chromatography with the CCl_4 as an internal standard. The polymer yield by gravimetry was in good agreement with the gas chromatographic conversion of the monomer.

To remove initiator and MX_n residues, the quenched reaction mixtures with **4**–$SnCl_4$ were washed with dilute hydrochloric acid, aqueous sodium hydroxide solution and then with water; those with **4**–$ZnCl_2$ were washed only with water. These solutions were evaporated to dryness under reduced pressure and vacuum dried to give the product polymers. The MWD of the polymers was measured by size-exclusion chromatography (SEC) in chloroform at room temperature on a Jasco Trirotar-V chromatograph equipped with three polystyrene gel columns (Shodex K-802, K-803 and K-804). The $\bar{M}_n$ and $\bar{M}_w/\bar{M}_n$ values were calculated from SEC eluograms on the basis of a polystyrene calibration.

^1H, ^{19}F and ^{13}C NMR spectroscopy and model reactions. ^1H, ^{19}F and ^{13}C NMR spectra were recorded on a JEOL JNM-GSX270 spectrometer, operating at 270·7 MHz (^1H NMR), 254·1 MHz (^{19}F NMR) and 67·9 MHz (^{13}C NMR) (CD_2Cl_2 for locking). The main parameters were as follows: ^1H NMR, spectral width = 6002·4 Hz (22·17 ppm), pulse width = 4·3 μs (45°), acquisition time + pulse delay = 30 s, data points = 16,384, number of transients = 8 (4 min for one spectrum); ^{19}F NMR, spectral width = 10,000·0 Hz (39·34 ppm), pulse width = 11·0 μs (45°), acquisition time + pulse delay = 30 s, data points = 16,384, number of transients = 12 (6 min for one spectrum); ^{13}C NMR (white-noise decoupled from ^1H), spectral width = 20,000·0 Hz (294·38 ppm), pulse width = 4·0 μs (45°), acquisition time + pulse delay = 3·0 s, data points = 32,768, number of transients = 500–2000 (30–120 min for one spectrum). The probe temperature was regulated with a JEOL NM-GVT3 variable-temperature apparatus (fluctuation ≤1 °C). The model reactions of **4** or **10** and Lewis acids (MX_n) were started by adding a solution of the adduct (1·0 M; 0·12 ml) to a prechilled CD_2Cl_2 solution of $SnCl_4$ or $ZnCl_2$ (0·48 ml) in a septum-capped NMR tube (5 mm o.d.) under dry nitrogen via dry syringes at −78 °C. For the reaction in the presence of a salt, it was dissolved in the solution of $SnCl_4$ beforehand. The tube was vigorously shaken at −78 °C and immediately placed in the thermostated probe. The chemical shifts in ^1H and ^{13}C NMR spectra were determined relative to the signals of the residual CH_2Cl_2 (^1H 5·32 ppm and ^{13}C 55·8 ppm, both from Me_4Si) in the deuterated solvent, and those in ^{19}F NMR spectra to the signal of trifluoromethylbenzene ($C_6H_5CF_3$; 64·0 ppm from $CFCl_3$) as an external standard dissolved in toluene-d_8 in a capillary. The interactions of $SnCl_4$ and/or nBu_4NCl with $nBu_4NOCOCF_3$ (**8**), $CF_3CO_2C_2H_5$ (**9**) and $AgOCOCF_3$ were analysed in a similar way by adding a solution of each acetate (0·12 ml; **8** in CD_2Cl_2; **9** in CCl_4; $AgOCOCF_3$ in toluene-d_8) to a prechilled solution of $SnCl_4$ (in CD_2Cl_2; 0·48 ml) at −78 °C.

ACKNOWLEDGEMENTS

We thank Professor Ken'ichi Takeuchi, Department of Energy and Hydrocarbon Chemistry, Kyoto University, for helpful discussions on NMR analysis. M.K. is also grateful to the Japan Society for the Promotion of Sciences for Fellowships for Japanese Junior Scientists.

REFERENCES

1. M. Kamigaito, H. Katayama, M. Sawamoto and T. Higashimura, *Polym. Prepr. Jpn., Engl. Ed.* **42** (2), E866 (1993).
2. M. Sawamoto, *Macromol. Symp.* **88**, 105 (1994).

3. (a) M. Szwarc, *Nature (London)* **178**, 1168 (1956); (b) M. Szwarc, M. Levy and R. Milkovich, *J. Am. Chem. Soc.* **78**, 2656 (1956).
4. (a) M. P. Dreyfuss and P. Dreyfuss, *Polymer* **6**, 93 (1965); (b) C. E. H. Bawn, R. M. Bell and A. Ledwith, *Polymer* **6**, 95 (1965).
5. M. Miyamoto, M. Sawamoto and T. Higashimura, *Macromolecules* **17**, 265, 2228 (1984).
6. For recent reviews, see (a) M. Sawamoto, *Prog. Polym. Sci.* **16**, 111 (1991); (b) J. P. Kennedy and B. Iván, *Designed Polymers by Carbocationic Macromolecular Engineering: Theory and Practice.* Hanser, Munich (1992); (c) M. Sawamoto, *Trends Polym. Sci.* **1**, 111 (1993).
7. See, for example: (a) P. Sigwalt, *Makromol. Chem., Macromol. Symp.* **47**, 179 (1991); (b) M. Szwarc, *Makromol. Chem., Rapid Commun.* **13**, 147 (1992); (d) K. Matyjaszewski, *J. Polym. Sci., Part A, Polym. Chem.* **31**, 995 (1993); *Macromolecules* **26**, 1787 (1993).
8. M. Kamigaito, M. Sawamoto and T. Higashimura, *Macromolecules* **25**, 2587 (1992).
9. M. Kamigaito, Y. Maeda, M. Sawamoto and T. Higashimura, *Macromolecules* **26**, 2670 (1993).
10. H. Katayama, M. Kamigaito, M. Sawamoto and T. Higashimura, *Macromolecules*, in press.
11. (a) M. Kamigaito, M. Sawamoto and T. Higashimura, *Macromolecules* **24**, 3988 (1991); (b) M. Kamigaito, K. Yamaoka, M. Sawamoto and T. Higashimura, *Macromolecules* **25**, 6400 (1992); (c) K. Matyjaszewski and C. H. Lin, *Makromol. Chem., Makromol. Symp.* **47**, 221 (1991); (d) J. E. Puskas, G. Kaszas and M. Litt, *Macromolecules* **24**, 5278 (1991).
12. F. G. Bordwell, *Acc. Chem. Res.* **21**, 456 (1988).